Computers and Concrete, *Vol. 17, No. 3 (2016) 387-406*
DOI: http://dx.doi.org/10.12989/cac.2016.17.3.387

Transverse reinforcement for confinement at plastic hinge of circular composite hollow RC columns

Deok Hee Won[1a], Taek Hee Han[1b], Seungjun Kim[2c], Woo-Sun Park[1d] and Young Jong Kang[*3]

[1]Coastal Engineering Division, Korea Institute of Ocean Science and Technology, Ansan 426-744, Republic of Korea
[2]Department of Geotechnical Disaster Prevention, Daejeon University, 62 Daehak-ro, Dong-gu, Daejeon 300-716, Republic of Korea
[3]Department of Architectural, Civil and Environmental Engineering, Korea University, 145 Anamro Seoul 156-701, Republic of Korea

(Received October 5, 2015, Revised December 22, 2015, Accepted January 25, 2016)

Abstract. Confined transverse reinforcement was arranged in a plastic hinge region to resist the lateral load that increased the lateral confinement effect in the bridge substructure. Columns increased the seismic performance through securing stiffness and ductility. The calculation method of transverse reinforcements at plastic hinges is reported in the AASHTO-LRFD specification. This specification was only proposed for solid reinforced concrete (RC) columns. Therefore, if this specification is applied for another column as composite column besides the solid RC column, the column cannot be properly evaluated. The application of this specification is particularly limited for composite hollow RC columns. The composite hollow RC column consists of transverse, longitudinal reinforcements, cover concrete, core concrete, and an inner tube inserted in the hollow face. It increases the ductility, strength, and stiffness in composite hollow RC columns. This paper proposes a modified equation for economics and rational design through investigation of displacement ductility when applying the existing specifications at the composite hollow RC column. Moreover, a parametric study was performed to evaluate the detailed behavior. Using these results, a calculation method of economic transverse reinforcements is proposed.

Keywords: transverse reinforcement; AASHTO; ductility; composite; hollow column

1. Introduction

Hollow reinforced concrete (RC) columns are used as economical design elements, because they use little material and are lightweight. However, they have poor ductility owing to brittle

*Corresponding author, Professor, E-mail: yjkang@korea.ac.kr
[a] Senior Research Scientist, E-mail: thekeyone@kiost.ac.kr
[b]Principal Research Scientist, E-mail: taekheehan@kiost.ac.kr
[c] Professor, E-mail: Rocksmell@gmail.com
[d]Principal Research Scientist, E-mail: wspark@kiost.ac.kr

http://www.techno-press.org/?journal=cac&subpage=8 ISSN: 1598-8198 (Print), 1598-818X (Online)

failure on the inner face of the column. The brittle failure of a hollow RC column originates from the lack of confinement of the core concrete, because, generally, the core concrete of a hollow RC column is confined only by the outer transverse reinforcements or both the outer and the inner transverse reinforcements. To prevent this brittle failure, Han *et al.* (2008) used an inner tube to reinforce the inner face of a hollow RC column as shown Fig. 1. This offered strong and durable confinement, because of the reinforcement provided by the inner tube. The column's strength and ductility were enhanced, because of the continuous confinement stress provided by the inner tube. This column has cover concrete on its outside but it does not has cover concrete on hollow section by inner tube. A nonlinear concrete model and the compressive performance of composite hollow RC column were evaluated through theoretical study and experimental study by Han *et al.* (2008, 2010). These studies considered the yielding and buckling failure conditions of the inner tube as well.

The confining transverse reinforcement was arranged in the plastic hinge region to resist the lateral load that increased the lateral confinement effect in the substructure of the bridge. This increased the seismic performance through securing the stiffness and ductility. A calculation method for confinement of transverse reinforcements is reported in the AASHTO-LRFD specification as shown Eq. (1). This specification suggested that the volumetric ratio of spiral or seismic hoop reinforcement shall satisfy either that required in Eq. (1a) and Eq. (1b). The Main function of transverse reinforcement specified in Eq. (1b) is to ensure that the axial load carried by the column after spalling of the concrete cover will at least equal the load carried before spalling and to ensure that bucking of the longitudinal reinforcement is prevent. Thus the spacing of the confining reinforcement is very important. However, this specification was only proposed for solid RC columns. Therefore, if this specification is applied to another column as composite column besides the solid RC column, this column cannot be properly evaluated. (Burak *et al.* 2014, Gholamreza *et al.* 2012, Kim 2014, Ou *et al.* 2012, and Song *et al.* 2011) In particular, composite hollow RC columns (Fig. 1) have limitations for applying this specification.

$$\rho_s = 0.45\left[\frac{A_g}{A_c} - 1\right]\frac{f_{ck}}{f_{yh}}, \text{ (AASHTO-LRFD 2012, 5.7.4.6)} \tag{1a}$$

$$\rho_s = 0.12\frac{f_{ck}}{f_{yh}}, \text{ (AASHTO-LRFD 2012, 5.10.11.4.1d)} \tag{1b}$$

where, A_g denotes the gross area of the column, A_c the area of the core concrete, f_{ck} the compressive strength of the concrete, and f_{yk} the strength of the transverse reinforcement.

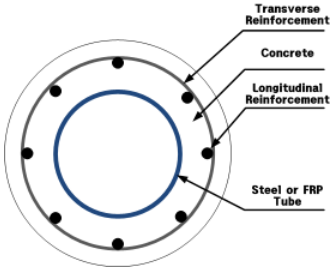

Fig. 1 Section of the composite hollow RC column

A composite hollow RC column consists of transverse and longitudinal reinforcement, cover concrete, core concrete, and an inner tube inserted in the hollow face. This increases the ductility, strength, and stiffness in a composite hollow RC column. This paper proposes a modified equation for economics and rational design of transverse reinforcements at a plastic hinge through investigation of displacement ductility when applying the existing specifications to a composite hollow RC column. Additionally, the proposed equation was verified under various conditions.

2. Background

Han *et al.* (2008, 2010), proposed the basic theory for the force-equilibrium condition and failure modes of a composite hollow RC column. In addition, they proposed a lateral force-displacement analysis method for this column.

2.1 Equilibrium in a composite hollow RC column (Han et al. 2008)

Han *et al.* (2008) defined the failure mode of a composite hollow RC column. Fig. 2 shows a half section of a composite hollow RC column when only an axial load acts on the concrete. Considering the failures of the inner tube and the transverse reinforcement, three failure modes could be defined, as shown in Eq. (2). In the first failure mode, the inner tube fails by buckling or yielding before the transverse reinforcement yields. The second failure mode is the reverse condition. In the third failure mode, the inner tube and transverse reinforcement fail simultaneously.

$$f_{tube} > f_{\lim} = smaller(f_{yt}, f_{bk}) : \text{Failure mode 1} \tag{2a}$$

$$f_{tube} < f_{\lim} = smaller(f_{yt}, f_{bk}) : \text{Failure mode 2} \tag{2b}$$

$$f_{tube} = f_{\lim} = smaller(f_{yt}, f_{bk}) : \text{Failure mode 3} \tag{2c}$$

where, f_{tube} is the stress acting on the inner tube in the radial direction (i.e., lateral pressure), f_{yt} the yield strength of the inner tube, f_{bk} the buckling strength of the inner tube, and $f_{\lim}$ the lower value between the yield and the buckling strength of the inner tube.

In the first failure mode, the concrete in the column was completely confined before the inner tube failed. After the inner tube failed, it was assumed to exert no more passive confining pressure. Therefore, after the inner tube failed, the concrete was under biaxial confinement. In the second failure mode, the concrete was completely confined until the entire column failed by yielding of the transverse reinforcement. The failure of the entire column depended on yielding of the transverse reinforcement. Because the triaxial confinement was completely maintained until the failure of the transverse reinforcement, the concrete in the column had strength equal to that in a solid RC column in this case. The confining pressure in the circumferential direction was equal to that in the radial direction ($f_{lc} = f_{lr} = f_l$). The third failure mode was very rare and it had a failure pattern similar to that of the second failure mode. Considering "failure mode 2" and "failure mode 3," Eqs. (3) and (4) can be derived from Fig. 2. By substituting Eq. (3) into Eq. (2), the confining pressure acting on the concrete was given as Eq. (5), where t is the thickness of the inner tube

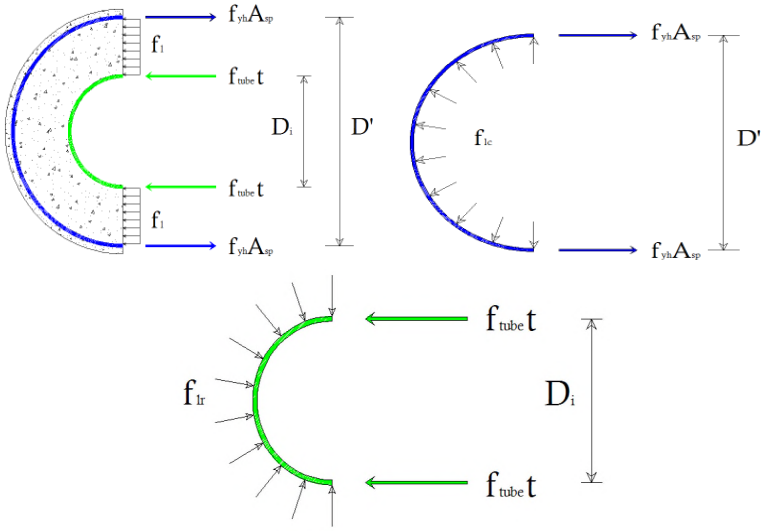

Fig. 2 Confinement stress on concrete in a composite hollow RC column (Han *et al.* 2008)

$$\{f_l(D'-D_i)+2f_{tube}t\}s=2f_{yh}A_{sp} \tag{3}$$

$$f_{tube}=\frac{f_lD_i}{2t},\ f_{lc}=f_{lr}=f_l \tag{4}$$

$$f_l=\frac{2f_{yh}A_{sp}}{D's} \tag{5}$$

2.2 Yielding condition of the inner tube

The yielding of an inner tube before the transverse reinforcement yields can be guaranteed by controlling the thickness of the inner tube. To avoid premature failure of the column, f_{lr} must be less than f_{yt}. The minimal thickness of the inner tube needed to prevent its premature yielding failure (t_{yt}) was calculated by Eq. (7).

$$f_{lr}=\frac{D_i\cdot f_{yh}\cdot A_{sp}}{D'\cdot s\cdot t}<f_{yt} \tag{6}$$

$$t_{yt}=\frac{D_i\cdot f_{yh}\cdot A_{sp}}{D'\cdot s\cdot f_{yt}} \tag{7}$$

2.3 Buckling condition of the inner tube (Han et al. 2008)

The inner tube of a composite hollow RC column is unilaterally restrained by concrete. Because of this unilateral boundary condition, the inner tube has a different buckling strength from

that of an arch or ring with bilateral conditions. The buckling strength of unilaterally restrained arches has been studied by many researchers. Kerr *et al.* (1969) proposed a method to determine the buckling strength of a circular arch by linearization of the pre-buckling deformation. Haftka *et al.* (1971) suggested a method to determine the bifurcation buckling strength and snap-through buckling strength of a circular shallow arch using Koiter's method. Sun *et al.* (1996) proposed the numerical solution of a large deformation problem by considering the unilateral boundary condition. The buckling behavior of the inner tube was considered the snap-through behavior of a circular shallow arch, because the inner tube can only buckle inward. The buckling coefficient proposed by Kerr *et al.* (1969) was adopted to estimate the buckling strength of the inner tube. From their study, the buckling strength of a circular shallow arch (p_o) can be calculated using Eq. (8). By substituting the snap-through buckling coefficient (2.27) for the normalized non-dimensional pressure ($\bar{p}$) in Eq. (8), the buckling strength of the inner tube (f_{bk}) can be calculated using Eq. (9).

$$p_o = \bar{p}\frac{EI}{R^2 t} \tag{8}$$

$$f_{bk} = 2.27\frac{EI}{R^2 t} = \frac{2.27}{3}\frac{t^2 E}{D_i^2} \tag{9}$$

where E is the modulus of elasticity, I the moment of inertia, and R the radius of the inner tube.

To prevent premature buckling failure of the inner tube before yielding of the transverse reinforcement, the buckling strength of the inner tube must be higher than the confining pressure acting on the concrete when the transverse reinforcement yields. With this design concept and Eq. (9), a failure criterion can be defined as Eq. (10). From Eq. (10), the required minimal thickness of the inner tube to prevent its premature buckling failure (t_{bk}) can be calculated using Eq. (11).

$$f_{bk} = \frac{2.27}{3}\frac{t^2 E}{D_i^2} > f_l = \frac{2 f_{yh} A_{sp}}{D's} \tag{10}$$

$$t_{bk} = \sqrt{\frac{6}{2.27}\frac{D_i^2 \cdot f_{yh} \cdot A_{sp}}{D' \cdot s \cdot E}} \tag{11}$$

The required minimal thickness of the inner tube to prevent its premature failure ($t_{\lim}$) can be defined as the higher value between t_{yt} and t_{bk} from Eqs. (7) and (11), respectively. When a composite hollow RC column fails by "failure mode 1," this failure mode can be classified into two failure modes. The first is failure by yielding of the inner tube. The other is failure by buckling of the inner tube. These failure modes can be determined by a comparison of the inner tube's yield strength (f_{yt}) and the buckling strength (f_{bk}). It is also possible to determine the failure mode with respect to a comparison of the thickness of the inner tube (t) and its required minimal thicknesses for yielding (t_{yt}) and buckling (t_{bk}).

2.4 Stress-strain relation

Han *et al.*'s (2008) concrete model was based on the unified concrete model proposed by Mander *et al.* (1984) who adopted Eq. (12) proposed by Popovics (1973) to develop the unified

$$f_c = \frac{f_{cc}^{'} xr}{r - 1 + x^r} \tag{12a}$$

$$x = \frac{\varepsilon}{\varepsilon_{cc}} \tag{12b}$$

$$r = \frac{E_c}{(E_c - E_{\sec})} \tag{12c}$$

$$E_{\sec} = \frac{f_{cc}^{'}}{\varepsilon_{cc}} \tag{12d}$$

stress–strain relation of confined concrete. This model is based on a constant confining pressure.

For triaxially confined concrete, the peak concrete strength was calculated with Eq. (13). For biaxially confined concrete, the peak concrete strength was calculated with Eq. (14) Han *et al*. (2008). The strain at the peak concrete strength was calculated with Eq. (15).

$$f_{cc}^{'} = f_c^{'}\left(2.254\sqrt{1 + \frac{7.94 f_l^{'}}{f_c^{'}}} - \frac{2 f_l^{'}}{f_c^{'}} - 1.254\right) \tag{13}$$

$$f_{cc}^{'} = -2.75\frac{f_{lc}^{'2}}{f_c^{'}} + 1.835 f_{lc}^{'} - f_c^{'} \tag{14}$$

$$\varepsilon_{cc} = \varepsilon_{co}\left[1 + 5\left(\frac{f_{cc}^{'}}{f_c^{'}} - 1\right)\right] \tag{15}$$

In an RC column, transverse reinforcements cannot confine the entire core concrete completely. Therefore, f_l should be replaced by f_l'. The effective constant confining pressure can be calculated by Eq. (16)

$$f_l^{'} = k_e f_l \tag{16}$$

2.5 Lateral load-displacement analysis method of column (Han et al.(2010))

To predict the behavior of a composite hollow RC column, a column analysis model was developed in this study based on Han *et al.*'s (2008) concrete model. This analysis tool is capable of axial load-bending moment interaction analyses and lateral load–displacement analyses. It used section analysis, accounting for equilibrium, strain compatibility, and material stress–strain curves and adopted the layer-by-layer technique for numerical integration of stress Han *et al.* (2010). The analyses were conducted for two conditions: (a) an unconfined concrete stress-strain curve with

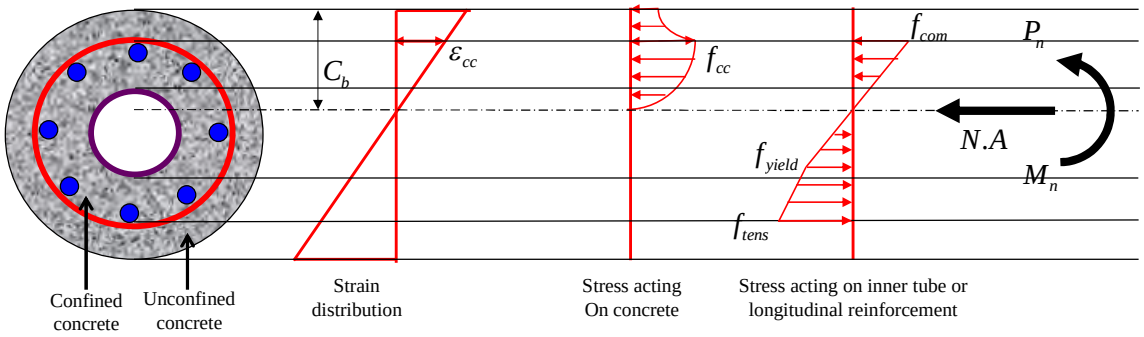

Fig. 3 Section analysis using strain compatibility and the layer-by-layer approach (Han *et al.* 2010)

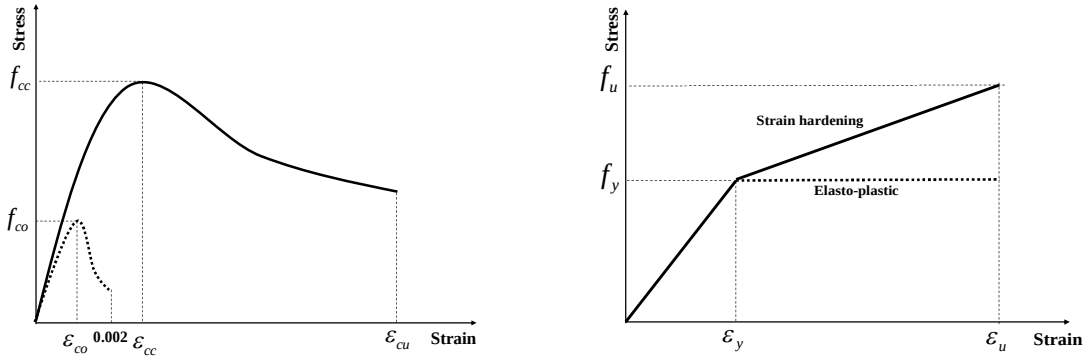

Fig. 4 Idealized stress-strain curves for (a) concrete and (b) steel (Han *et al.* 2010)

elasto-plastic steel behavior and (b) a confined concrete stress-strain curve and accounting for strain hardening of the steel. Fig. 3 shows an idealized section. Fig. 4 shows the adopted stress–strain curves. The analyses were performed at the stage of strain distribution as shown in Fig. 5. For each stage of strain distribution, stresses acting on the concrete, the longitudinal reinforcements, and the inner tube were calculated. By summing them, the axial load and the moment were calculated for each stage of the strain distribution. P_j, M_j and ϕ_j are given by Eqs. (17-19), respectively.

$$P_j = P_j^{CC} + P_j^{CV} + P_j^R + P_j^T \tag{17}$$

$$M_j = M_j^{CC} + M_j^{CV} + M_j^R + M_j^T \tag{18}$$

$$\phi_j = \frac{\varepsilon_{cc}}{C_{b,j}} \tag{19}$$

Lateral forces and lateral displacements can be calculated with the determined moments and curvatures at the corresponding stage of the strain distribution. $F_{L,j}$ was simply determined by Eq. (20). However, more calculations were required to determine the lateral displacement from the curvature. ϕ_P is the difference between ϕ_u and ϕ_y, as given by Eq. (21). The plastic curvature was

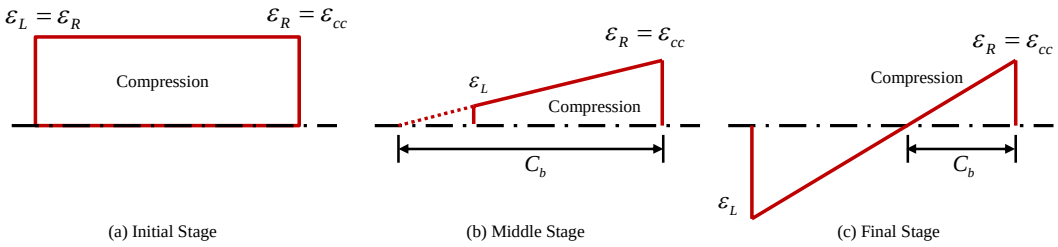

Fig. 5 Stages of strain distribution at the (a) initial, (b) middle, and (c) final stage (Han *et al.* (2010))

assumed constant over the equivalent plastic hinge length, which was calibrated to give the same plastic rotation as occurred in the real column. From the analyses and test results by Priestly *et al.* (1996), a reasonable estimate, given by Eq. (22), was made for the plastic hinge length when the plastic hinge formed against a supporting member (such as in Fig. 6). Here, f_{ye} is yield strength of longitudinal reinforcements.

$$F_{L,j} = \frac{M_j}{L} \tag{20}$$

$$\phi_P = \phi_u - \phi_y \tag{21}$$

$$L_P = 0.8L_H + 0.022\, f_{ye} d_{bl} \geq 0.044\, f_{ye} d_{bl} \,(f_{ye}\, in\, MPa) \tag{22}$$

The second term in Eq. (22) makes allowance for additional rotation at the critical section resulting from strain penetration of the longitudinal reinforcement into footing. The plastic rotation is given by Eq. (23). Excluding all additional flexibility effects, the yield displacement can be approximated by Eq. (24). The plastic displacement (Δ_P) includes the component owing to the plastic rotation (θ_P) and additional elastic displacement from the nominal moment capacity (M_n) to the maximum moment capacity (M_u). The plastic displacement is given by Eq. (25). Using derived equations, a column analysis program was coded in the FORTRAN language.

$$\theta_P = L_P \phi_P = L_P \left(\phi_u - \phi_y\right) \tag{23}$$

$$\Delta_y = \frac{\phi_y L_H^2}{3} \tag{24}$$

$$\Delta_P = \left(\frac{M_u}{M_n} - 1\right)\Delta_y + L_P \phi_P \left(L - 0.5L_P\right) \tag{25}$$

This method was verified through the experimental study by Han *et al.* (2010). These analyses results showed acceptable agreement with the test results. It showed that the developed model is reasonable and that the confining effect of concrete must be considered to predict the behavior of a composite hollow RC column. This study estimated the displacement ductility of a composite hollow RC column using Han *et al.*'s method.

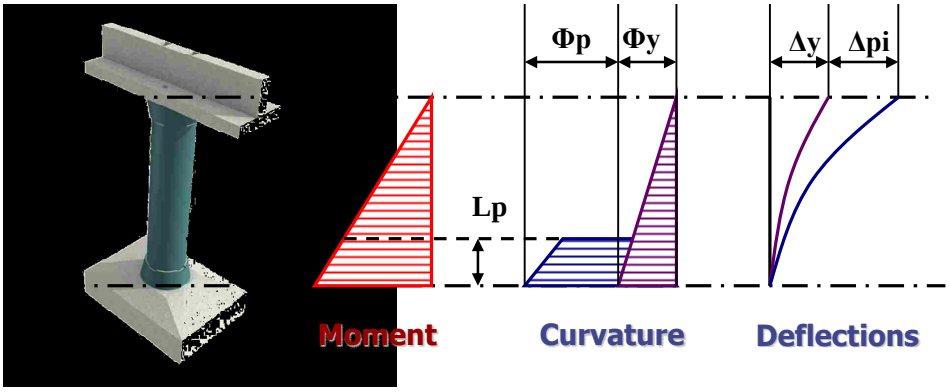

Fig. 6 Inelastic deformation of a column (Han *et al.* 2010)

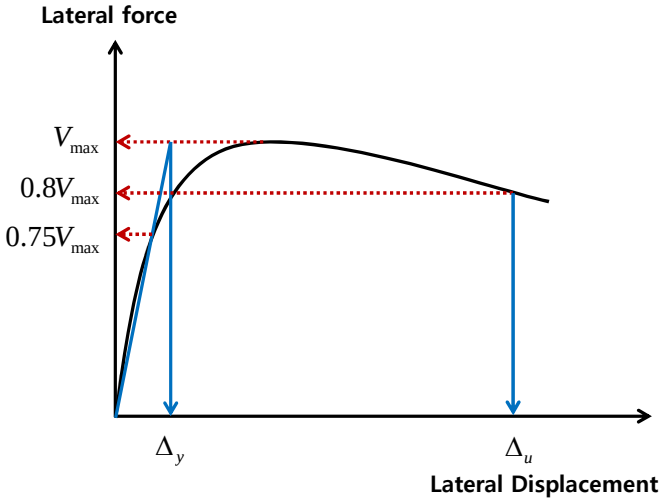

Fig. 7 Defined method of displacement ductility (Park 1988)

3. Ductility ratio of a circular composite hollow RC column according to the AASHTO-LRFD specification

This section studies change of ductility by geometric section properties of composite hollow RC column. Parameters are the hollow ratio, diameter, and thickness of the inner tube. Change effect of ductility by Transverse and longitudinal reinforcements in this column was investigated by Won *et al.* (2012)

The displacement ductility of a composite hollow RC column was evaluated by varying the hollow ratio, diameter, thickness of the inner tube, and axial force. The confining transverse reinforcements of a composite hollow RC column were calculated using the AASHO-LRFD specification as in Eq. (1). Here, the core concrete of a composite hollow RC column was confined by the inner tube and transverse reinforcements. The material model of this column was the same as that of a solid RC column when transverse reinforcement reached to failure before yield failure or buckling of the inner tube. Therefore, the gross area (A_g) and the core concrete area (A_c) of the

Table 1 Dimensions of the column model

Spec.	Dimension
Diameter	2,500.0
Thickness of cover concrete	60.0
longitudinal rebar ratio	0.011
min. transverse rebar ratio	0.0072
slenderness ratio	23.0
strength of concrete	21
yield strength of rebar	350
yield strength of internal tube	235
Elastic modulus of steel	210,000
Elastic modulus of rebar	200,000
Elastic modulus of concrete	26,115

Table 2 Section dimensions according to the hollow ratio

Hollow ratio	Diameter of hollow section	Thickness of inner tube
0.0	-	-
0.2	473.2	1.4
0.4	952.0	2.7
0.5	1183.2	3.4
0.6	1419.8	4.1
0.7	1656.6	4.7
0.8	1892.0	6.0
0.9	2113.6	14.2

composite hollow RC column should be considered as an area confined by transverse reinforcements that includes a hollow part.

$$\mu_{\Delta} = \frac{\Delta_u}{\Delta_y} \tag{26}$$

Fig. 7 shows the defined method of displacement ductility. Displacement ductility was calculated by the ratio of yield displacement and ultimate displacement as in Eq. (26). Here, Δ_u is the ultimate displacement and Δ_y the yield displacement.

Hollow ratio

The hollow ratio is inside diameter of outside diameter of confined concrete in composite hollow RC column. To investigate displacement ductility by hollow ratio, dimensions of a composite hollow RC column were selected as in Table 1 and 2. Table 1 shows the common dimensions of the analysis models and Table 2 the dimensions of the inner tube and hollow part according to the hollow ratio. Hollow ratios were considered from 0.0 to 0.9 and the thickness of the inner tube was selected by Eqs. (7) and (11) (Table 2).

Fig. 8 shows the change in displacement ductility by hollow ratio in the composite hollow RC

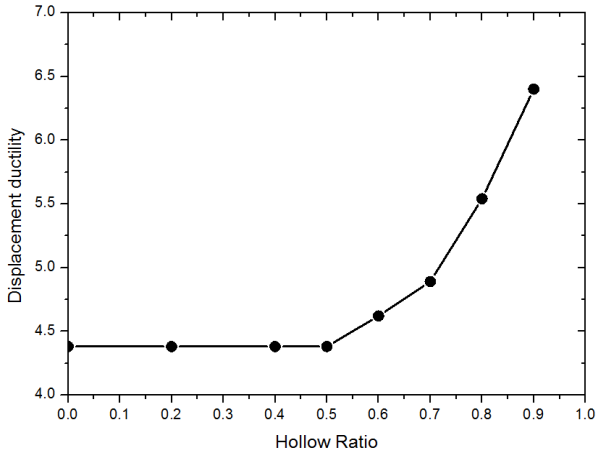

Fig. 8 Change in displacement ductility by hollow ratio in the composite hollow RC column

Table 3 Material model of the columns

	Strain at peak stress	Peak Axial Stress(MPa)	Ultimate Strain
0.0	0.0055	28.3428	0.0239
0.2	0.0055	28.3544	0.0239
0.4	0.0055	28.3652	0.0239
0.5	0.0055	28.3710	0.0239
0.6	0.0055	28.3768	0.0239
0.7	0.0055	28.3818	0.0239
0.8	0.0055	28.3877	0.0239
0.9	0.0055	28.3935	0.0239

Table 4 Section dimensions according to hollow ratio

Thickness of inner tube	0.0	5.4	6.0	6.5	7.0	7.5	8.0	8.5
Displacement ductility	4.6	5.5	5.5	5.5	5.5	5.5	5.5	5.5

** Dimensions of columns are same hollow ratio 0.8 model.

column. The displacement ductility of the analysis model increased rapidly from a hollow ratio of 0.5. When the hollow ratio was 0.9, the displacement ductility was about 6.5. The displacement ductility at a hollow ratio of 0.9 was 30% larger than that of the solid RC column with a hollow ratio of 0.0. Table 3 shows the material model of the confined concrete. The strain of peak stress, peak axial stress, and ultimate strain had the same values. This showed that a parameter existed that affected the change in ductility, except the performance of confining concrete.

Thickness of the inner tube

Next, thickness of the inner tube at a hollow ratio of 0.8 was changed to investigate the effect of the inner tube thickness against displacement ductility. Table 4 shows the displacement ductility versus the thickness of the inner tube. For these analyses, the analysis models were considered the same model with a hollow ratio of 0.8 and the thickness of the inner tube changed from 0 to 8.5

Table 5 Analysis model by column diameter

	Hollow ratio	Longitudinal rebar ratio	Transverse rebar ratio
D700	0.0~0.9	0.011	0.0072
D1000	0.0~0.9	0.011	0.0072
D2000	0.0~0.9	0.011	0.0072
D2500	0.0~0.9	0.011	0.0072
D3000	0.0~0.9	0.011	0.0072
D3500	0.0~0.9	0.011	0.0072

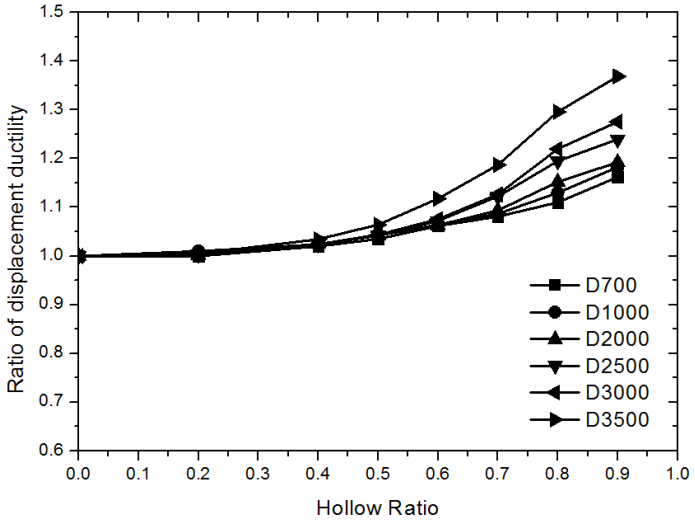

Fig. 9 Ratio of displacement ductility by column diameter

mm. The analysis results showed that the displacement ductility had a value of 5.5 except the model of 1 mm thickness of inner tube. When column don't have inner tube, displacement ductility is reduced because confined concrete become biaxial confinement state. If the inner tube has over necessary thickness, it doesn't affect the change in displacement ductility (Table 4).

Column Diameter

Next, the change in displacement ductility was investigated with the column diameter. Table 5 shows that the column diameter changed from 700 to 3500 mm and the hollow ratio from 0.0 to 0.9. The longitudinal reinforcement ratio, transverse reinforcement ratio, and slenderness ratio were the same on all models.

Fig. 9 shows the ratio of ductility of displacement by column diameter. When the column diameter increased, the ratio of displacement ductility increased. The displacement ductility of the composite hollow RC column was highly affected by change in the diameter and hollow ratio under the same conditions of transverse reinforcement, longitudinal reinforcement, and slenderness ratio.

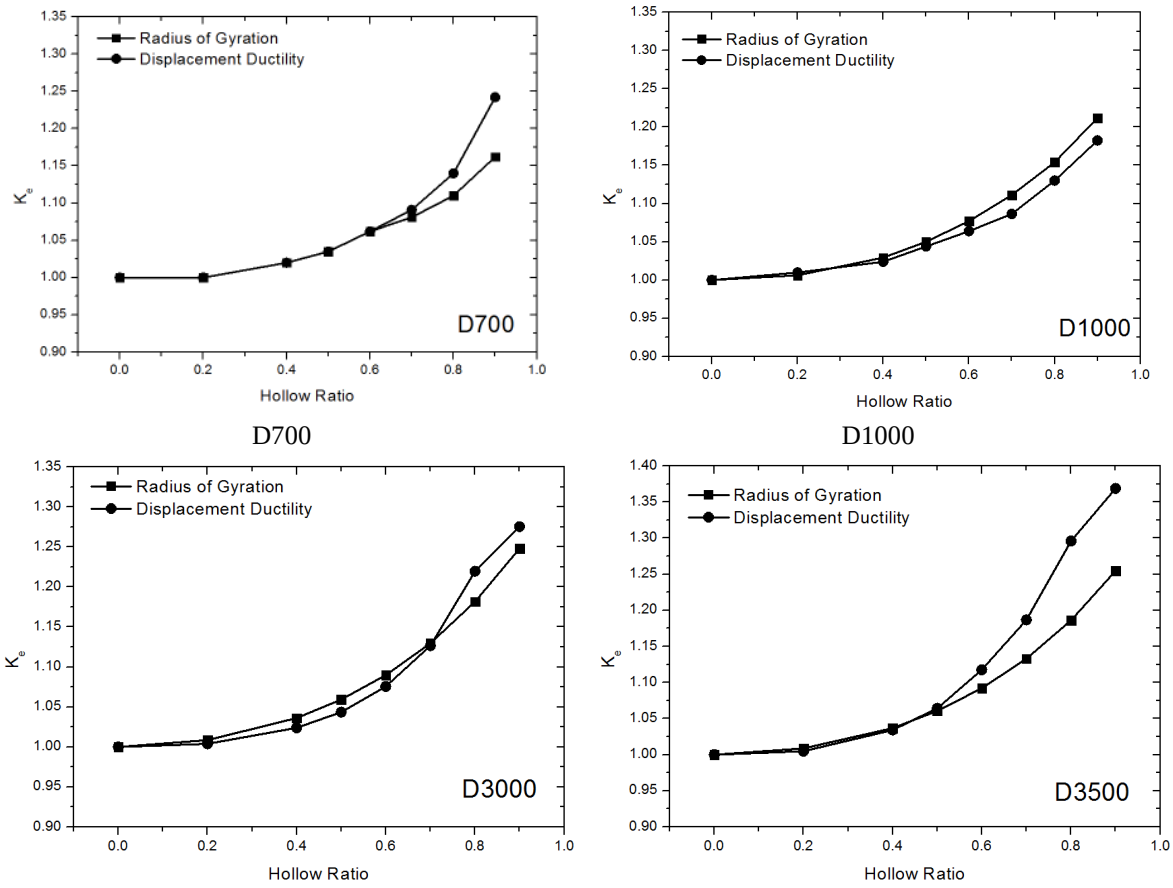

Fig. 10 Ratio of displacement ductility and radius of gyration for different column diameters

4. Modified equation for confining the transverse reinforcements of the circular composite hollow RC column

Parametric studies showed that the hollow ratio and diameter of the composite hollow RC column affected the change in displacement ductility more than other parameters. Changes in the hollow ratio and column diameter meant changes in the sectional shape of the composite hollow RC column. Therefore, the sectional shape of the column estimated to effect the change in displacement ductility. The relationship between the radius of gyration and the displacement ductility were investigated by comparing them. The radius of gyration of the composite section could be calculated by Eq. (27) using ACI code (318-08).

$$r = \sqrt{\frac{0.2E_cI_g + E_sI_s}{0.2E_cA_g + E_sA_s}} \tag{27}$$

where, E_c denotes the elastic modulus of concrete, E_s the elastic modulus of the steel tube, I_s the

Table 6 Transverse reinforcement at the plastic hinge calculated by the modified equation

	ρ_s	γ	Thickness of inner tube
0.0	0.007	-	-
0.2	0.007	0.981	1.4
0.4	0.006	0.921	2.6
0.5	0.006	0.878	3.2
0.6	0.005	0.825	3.7
0.7	0.005	0.765	4.2
0.8	0.005	0.697	4.5
0.9	0.004	0.624	4.8

moment of inertia of the steel tube, I_g the moment of inertia of the gross area, A_g the gross area, and A_s the area of the steel tube.

Fig. 10 shows the relationship between the ratio of displacement ductility and the radius of gyration. They were not perfect, but they had a similar tendency to increase. Here, K_e denotes the ratio based on a hollow ratio of 0.0.

A modified equation was suggested for the calculation of transverse reinforcement at a plastic hinge of a composite hollow RC column that used the relationship between the displacement ductility and the radius of gyration. A goal of this modified equation was a composite hollow RC column with similar displacement ductility as a solid RC column. This method could be induced by economic design of a composite hollow RC column. Here, we imposed the reduction coefficient, γ, that can be calculated with Eq. (29).

$$\gamma \cdot \left(\rho_s = l\arg er\left(0.45\left[\frac{A_g}{A_c} - 1 \right] \frac{f_{ck}}{f_{yh}}, 0.12\frac{f_{ck}}{f_{yh}} \right) \right) \tag{28}$$

$$\gamma = \left(\frac{r_s}{r_x} \right)^{\alpha} \tag{29}$$

$$\alpha = 1.108\ln D - 6.659 \tag{30}$$

where γ denotes the reduction coefficient, r_s the radius of gyration of the solid RC column, r_x the radius of gyration of the composite hollow RC column, and D the diameter of the column.

Table 6 shows the transverse reinforcement ratio at the plastic hinge calculated by the proposed equation. The transverse reinforcement ratio at the plastic hinge decreased from 0.007 to 0.004 at a hollow ratio of 0.9.

These results lead to decreased ductility of displacement (Fig. 11). The displacement ductility of a composite hollow RC column had a steady value by hollow ratio like a solid RC column. The displacement ductility was reduced reasonably. Reduction of reinforcement at the plastic hinge led to increased construction ability, as well as economics.

Table 7 shows the reduction ratio of the transverse reinforcements and the thickness of the inner tube of the modified models in contrast to the AASHTO specification. The transverse reinforcement ratio at the plastic hinge decreased 2.8-38.9%. In addition, the thickness of the inner

Table 7 Reduction ratio of the modified models in contrast with the existing specification

	Comparison	
	Transverse reinforcement ratio	Thickness of inner tube
0.0	0.0%	-
0.2	2.8%	0.0%
0.4	8.3%	3.7%
0.5	12.5%	5.9%
0.6	18.1%	9.8%
0.7	23.6%	10.6%
0.8	30.6%	16.7%
0.9	38.9%	21.3%

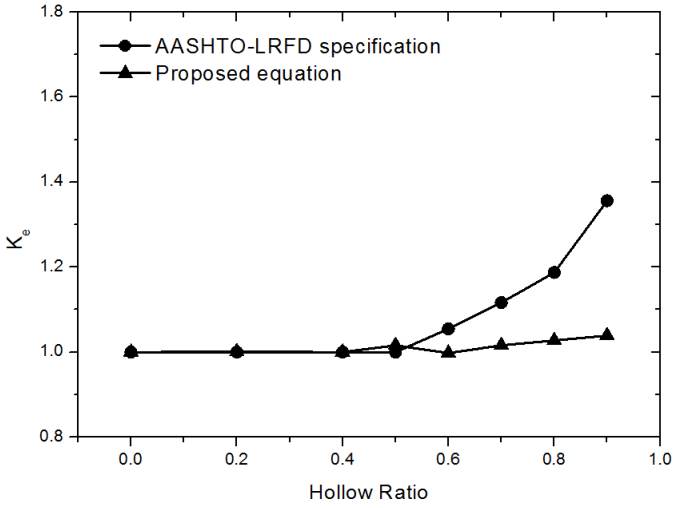

Fig. 11 Comparison of the displacement ductility ratio and the AASHO-LRFD specification

tube decreased 3.7-21.3%.

The proposed equation must have similar results under various conditions of diameter, hollow ratio, strength of transverse reinforcement, and compressive strength of the concrete. The proposed equation was verified through these parametric studies. Table 7 shows the dimensions of the analysis model. The diameter was changed between 700 and 4,000 mm. Compressive strength of the concrete was changed between 21 and 30 MPa. The strength of the transverse reinforcements was selected between 300 and 500 MPa. Each model had a transverse reinforcement ratio and thickness of the inner tube by hollow ratio. Also, Change of displacement ductility by axial force is evaluated. Axial force is acting on top of column. Acting axial force is selected 10%~40% of total section force. Dimensions of these models are same D2500 models.

Figs. 12-15 show the ratio of displacement ductility by each variable. All variables had larger displacement ductility than the solid RC column. The proposed equation had reasonable results for various conditions; it would enable design of transverse reinforcement at the plastic hinge on a composite hollow RC column.

Table 8 Dimensions of the analysis models

		Transverse reinforcement ratio	Thickness of inner tube
Diameter	D700	0.0123~0.01221	0.6～2.2
	D1500	0.0072~0.00527	0.8～3.0
	D2000	0.0072~0.00482	1.1～4.0
	D2500	0.0072~0.00449	1.4～4.8
	D3000	0.0072~0.00423	1.7～5.7
	D3500	0.0072~0.00403	1.9～6.5
	D4000	0.0072~0.00386	2.2～7.3
Compressive strength of concrete	21 MPa	0.0072~0.00449	1.4～4.8
	24 MPa	0.0082~0.00514	1.5～5.2
	27 MPa	0.0092~0.00579	1.7～5.5
	30 MPa	0.0102~0.00645	1.8～5.8
Strength of transverse reinforcement	300 MPa	0.0084~0.00524	1.4～4.8
	350 MPa	0.0072~0.00449	1.4～4.8
	400 MPa	0.0063~0.00393	1.4～4.8
	500 MPa	0.0050~0.00314	1.4～4.8
Axial Force	0%	0.0072~0.00449(D2500)	1.4～4.8
	10%	0.0072~0.00449(D2500)	1.4～4.8
	20%	0.0072~0.00449(D2500)	1.4～4.8
	30%	0.0072~0.00449(D2500)	1.4～4.8
	40%	0.0072~0.00449(D2500)	1.4～4.8

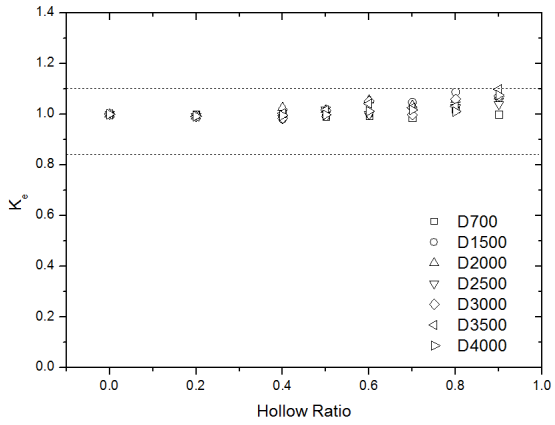

Fig. 12 Ratio of displacement ductility by column diameter

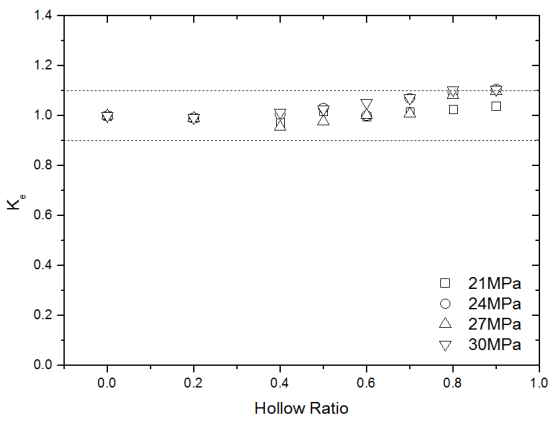

Fig. 13 Ratio of displacement ductility by compressive strength of the concrete

5. Results and summary

This study investigated transverse reinforcement at a plastic hinge on a composite hollow RC

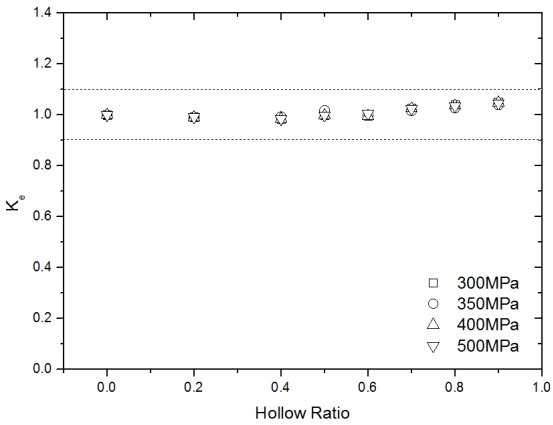

Fig. 14 Ratio of displacement ductility by strength of the transverse reinforcement

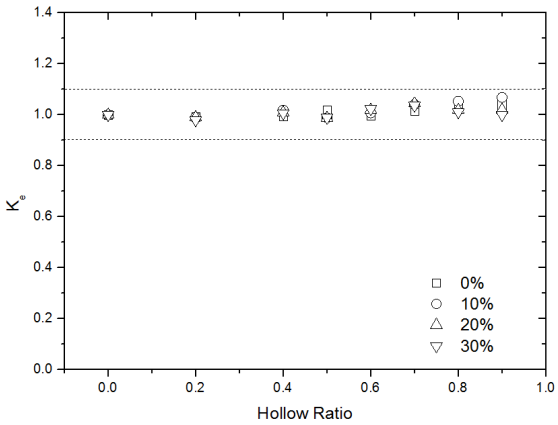

Fig. 15 Ratio of displacement ductility by axial force

column. A modified equation was proposed for economics and rational design, through investigation of displacement ductility when applying the AASHTO specification to a composite hollow RC column. Additionally, a parametric study was performed to evaluate the detailed behavior. The relation of the radius of gyration and displacement ductility of a composite hollow RC column was derived. They had similar tendencies. Using these results, the calculation method of economic transverse reinforcement at a plastic hinge was proposed. The proposed equation had reasonable results for various conditions; it would enable design of transverse reinforcement at a plastic hinge on a composite hollow RC column.

Acknowledgements

This research was supported by a grant(code NRF-2011-355-D00066) from National Research Foundation of Korea and a grant (code 12 Technology Innovation E09) from the Construction Technology Innovation Program funded by the Ministry of Land, Transportation Affairs (MLTM) of the Korean government.

References

AASHTO, LRFD (2007), Bridge Design Specifications, *American Association of State Highway and Transportation Officials*, SI Unit, 3rd Edition, Washington, DC, USA.

ACI Committee, American Concrete Institute and International Organization for Standardization (2008), *Building code requirements for structural concrete (ACI 318-08) and commentary*, American Concrete Institute.

Burak, Y. and Yusuf, C. (2014), "Effects of confinement reinforcement and concrete strength on nonlinear behaviour of RC buildings", *Comput. Concrete*, **14**(3), 279-297.

Gholamreza, G.A., Azadeh, J.J. and Benyamin, M. (2012), "Determination of plastic hinge properties for static nonlinear analysis of FRP-strengthened circular columns in bridges", *Comput. Concrete*, **10**(5), 435-

455.
Haftka, R.T., Mallet, R.H. and Nachbar, W. (1971), "Adaptation of Koiter's method to finite element analysis of snap-through buckling behaviour", *Int. J. Solid Struct.*, **10**, 1427-1445.
Han, T.H., Lim, N.H., Han, S.Y., Park, J.S. and Kang, Y.J. (2008), "Nonlinear concrete model for an internally confined hollow reinforced concrete column", *Mag. Concre Res.*, **60**(6), 429-40.
Han, T.H., Stallings, J.M., Cho, S.K. and Kang, Y.J.(2010), "Behaviour of a hollow RC column with an internal tube", *Mag. Concrete Res.*, **62**(1), 25-38.
Han, T.H., Yoon, K.Y. and Kang, Y.J. (2010), "Compressive strength of circular hollow reinforced concrete confined by an internal steel tube", *Constr. Build. Mater.*, **24**(9), 1690-1699.
Kerr, A.D. and Soifer, M.T. (1969), "The linearization of the prebuckling state and its effects on the determined instability load", *J. Appl. Mech.*, **36**(4), 775-785.
Kilpatrick, A.E. and Ranagan, B.V. (1997), "Deformation-control analysis of composite concrete columns", Research Report No. 3/97, School of Civil Engineering, Curtin University of Technology, Perth, Western Australia.
Kim, T.H. (2014), "Structural performance assessment of deteriorated reinforced concrete bridge piers", *Comput. Concrete*, **14**(4), 387-403.
Mander, J.B., Priestly, M.J.N. and Park, R. (1984), "Seismic design of bridge piers", Research Report No. 84-2, University of Canterbury, New Zealand.
Ou, Y.C., Kurniawan, R.A., Kurniawan, D.P. and Nguyen, N.D. (2012), "Plastic hinge length of circular reinforced concrete columns", *Comput. Concrete*, **10**(6), 663-681.
Park, R. (1988), "Ductility evaluation from laboratory and analytical testing", *Proceedings of the 9th World Conference on Earthquake Engineering*, Tokyo, **8**, 605-616.
Popovics, S. (1973), "A numerical approach to the complete stress-strain curves of concrete", *Cement Concrete Res.*, **3**(5), 583-599.
Priestley, M.J.N., Seible, F. and Calvi, G.M. (1996), *Seismic design and retrofit of bridges*, Wiley, New York.
Song, Z. and Lu, Y. (2011), "Numerical simulation of concrete confined by transverse reinforcement", *Comput. Concrete*, **8**(1), 23-41.
Sun, S.M. and Natori, M.C. (1996), "Numerical solution of large deformation problems involving stability and unilateral constraints", *Comput. Struct.*, **58**(6), 1245-1260.
Won, D.H, Han, T.H., Kim, J.H., Choi, J.H. and Kang, Y.J.(2012), "A parametric study on seismic performance of internally confined hollow RC columns", *J. Korea Soc. Adv. Comp. Struct.*, **3**(2), 28-35.

CC

Notation

A_{sp} area of transverse reinforcement
A_g gross area of the column,
A_c area of the core concrete,
D' outside diameter of the confined concrete
D_i inside diameter of the confined concrete
D Diameter of the column.
E modulus of elasticity
E_c tangent modulus of unconfined concrete

E_{sec} tangent modulus of confined concrete
I moment of inertia
f_c stress acting on concrete
$f_c^{'}$ strength of unconfined concrete
$f_{cc}^{'}$ confined strength of concrete
f_{ck} compressive strength of the concrete, and
f_{ye} yield strength of the longitudinal reinforcement.
f_{yh} yield strength of the transverse reinforcement.
f_{tube} stress acting on the inner tube in the radial direction (i.e., lateral pressure),
f_{yt} yield strength of the inner tube,
f_{bk} buckling strength of the inner tube, and
f_{lim} Lower value between the yield and the buckling strength of the inner tube.
f_l confining stress
f_{lc} confining pressure in the circumferential direction
f_{lr} confining pressure in the radial direction
k_e reduction coefficient for the effective constant lateral confining pressure
L height of the column
L_H distance from the critical section of the plastic hinge to the point of contrat flexure
L_P length of the equivalent plastic hinge
M_o nominal moment without axial load
M_b nominal moment under balanced condition
M_J moment at the jth stage of the strain distribution
M_j^{cc} moment acting on core concrete at the jth stage of the strain distribution
M_j^{cv} moment acting on cover concrete, at the jth stage of the strain distribution
M_j^R moment acting on longitudinal reinforcements at the jth stage of the strain distribution
M_j^T moment acting on the internal tube at the jth stage of the strain distribution
M_n nominal moment capacity of the column
M_u maximum moment capacity of the column
P_o nominal axial strength without eccentricity
P_b nominal axial strength under balanced condition
P_j axial load at the jth stage of the strain distribution
P_j^{CC} axial load acting on core concrete at the jth stage of the strain distribution
P_j^{CV} axial load acting on cover concrete at the jth stage of the strain distribution
P_j^R axial load acting on longitudinal reinforcements at the jth stage of the strain distribution
P_j^T axial load acting on internal tube at the jth stage of the strain distribution

p_o buckling strength of a circular shallow arch
$\overline{p}$ normalized nondimensional pressure
Q_y yield strength of the column under static state
R radius of the inner tube
r_s the radius of gyration of the solid RC column,
r_x the radius of gyration of the composite hollow RC column
s space of transverse reinforcement
t_{bk} thicknesses for buckling
t_y minimal required thickness of inner tube
t_{yt} thicknesses for yielding
ρ_s ratio of spiral or seismic hoop reinforcement
Δ_p plastic displacement of the column
Δ_y yield displacement of the column
ε axial strain of concrete
ε_{cc} axial strain of concrete at its peak strength
ε_{co} axial strain of unconfined concrete at its peak strength
ε_{cu} ultimate strain of the concrete
ε_u ultimate strain of the steel tube or the reinforcement
ε_L left side strain of section
ε_R right side strain of section
ε_y yield strain of the steel tube or the reinforcement
θ_p plastic rotation of the column
φ_j curvature of the column at the jth stage of the strain distribution
ϕ_P plastic curvature capacity
ϕ_u ultimate curvature corresponding to the ultimate strain of the concrete
ϕ_y yield curvature
γ denotes the reduction coefficient